IEEE Access
Multidisciplinary | Rapid Review | Open Access Journal

Received January 16, 2020, accepted January 30, 2020, date of publication February 4, 2020, date of current version February 11, 2020.

Digital Object Identifier 10.1109/ACCESS.2020.2971649

Approximate Dynamic Inversion for Nonaffine Nonlinear Systems With High-Order Mismatched Disturbances and Actuator Saturation

HAO YANG AND HAILONG PEI

Key Laboratory of Autonomous Systems and Networked Control, Ministry of Education, Unmanned Aerial Vehicle Systems Engineering Technology Research Center of Guangdong, South China University of Technology, Guangzhou 510640, China

Corresponding author: Hailong Pei (auhlpei@scut.edu.cn)

This work was supported in part by the Scientific Instruments Development Program of NSFC under Grant 615278010, and in part by the Science and Technology Planning Project of Guangdong, China, under Grant 2017B010116005.

ABSTRACT In this paper, a novel disturbance-observer-based approximate dynamic inversion (ADI) approach is developed for pure-feedback nonaffine-in-control nonlinear systems (PFNNSs) in the presence of both high-order mismatched disturbances and actuator saturation. Finite-time disturbance observers (FTDOs) are utilized to estimate the disturbances and their derivatives. Then, we rebuild the system with the outputs of FTDOs. Thereafter, ADI is employed to derive the desired virtual and actual control of the nominal system, where no disturbances and saturation are presented. Furthermore, an augmented intermediate subsystem is constructed for the reduced slow subsystem to compensate for the difference between inputs with and without saturation by approximating its inversion. The stability of the closed-loop system is studied using Tikhonov's theorem. The proposed method is applied to a numerical example and a one-link robotic system with a brush DC motor. The simulation results demonstrate the validity of the presented approach.

INDEX TERMS High-order mismatched disturbances, actuator saturation, finite-time disturbance observer, approximate dynamic inversion, singular perturbation theory.

I. INTRODUCTION

High-order mismatched disturbances are frequently encountered in control system design, such as wheeled inverted pendulums [1], magnetic levitation suspension vehicles [2], and robotic manipulators [3], etc. The presence of high-order mismatched disturbances has to be explicitly taken into consideration to design robust and high-performance tracking schemes. On the other hand, actuator saturation is a common issue in a number of practical systems, such as surface vessels [4], robotic manipulators [5], and unmanned hydraulic systems [6], etc. The appearance of actuator saturation may lead to degradation of transient performance or destabilizing the system [7]. Thus, the development of control schemes for nonlinear systems with high-order disturbances and actuator saturation has been considered as one of the most challenging and attractive topics.

Up to present, many elegant control approaches, such as H_∞ control [8], sliding mode control (SMC) [9], and backstepping based method [10] have been proposed for mismatched disturbances attenuation. Although the previous methods have proved to be efficient, they handle the disturbances in a robust way, which suggests that the disturbance-rejection is obtained at the cost of nominal performance [11]. The disturbance-observer-based control (DOBC) approach can attenuate the disturbances through a faster dynamic response [12]. Moreover, the feed-forward control component of DOBC methods can directly compensate for disturbances in the system. Thus, DOBC schemes are able to achieve the robustness of the closed-loop system without conflicting requirements between control performance [2]. In [13], a high-order sliding mode differentiator is presented to estimate disturbances with high robustness and finite-time convergent performance. Recently, finite-time disturbance observers (FTDOs) have been widely investigated in the literature for nonlinear systems in the presence of high-order mismatched disturbances. In [14], researchers develop an FTDOs based SMC method to drive the system output to the desired set-point asymptotically. In [11], a baseline feedback control law is proposed with FTDOs for a class

The associate editor coordinating the review of this manuscript and approving it for publication was Bing Li.

of nonlinear systems, whose nominal systems are feedback linearizable. In [15], Fang and Liu employ an FTDOs based continuous nonsingular terminal SMC scheme for a small-scale helicopter with high-order mismatched disturbances. Nevertheless, the disturbance-attenuation methods in [11], [13]–[15] mainly focus on the affine-in-control nonlinear systems, which limits the application scope of FTDOs.

The actuator saturation problem has gained a great amount of attention during the past decades. Many studies have focused on stability analysis of the control systems under input saturation [16], [17], and extensive control schemes have been developed. In [18], a fault tolerant controller is designed for a class of uncertain networked control systems under actuator saturation. In [19], the authors introduce a H_∞ output-feedback strategy for vehicle lateral dynamics subjected to network-induced delay and tire force saturation. In [20], Aouaouda and Chadli develop a fault tolerant constrained control method for a class of Takagi-Sugeno systems under actuator saturation and state constraints. In [21], a composite nonlinear feedback control design is proposed for input saturated strict-feedback nonlinear systems.

However, to the best of our knowledge, the systems are required to be affine-in-control to implement the aforementioned methods. Nonaffine-in-control nonlinear systems are very common in practical engineering, such as flight vehicles [22], hypersonic vehicles [23], and electromechanical systems [24]. Some of the studies for nonaffine nonlinear systems have utilized the neural network and fuzzy control based methods, such as adaptive neural control [25], [26], adaptive fuzzy control [27], adaptive neural dynamic surface control [28], etc. Nevertheless, the heavy computational burdens resulting from adaptive fuzzy or neural weights are unacceptable in practical implementation [24].

Singular perturbation theory (SPT) is considered as an effective method for multiple time-scale systems. Recently, it has been adopted for various kinds of nonlinear control problems. In [29], semi-global practical stability of the closed-loop system under dynamic surface control scheme is studied by SPT. In [30], the authors employ SPT to design acceleration estimator for multiple vehicles. In [31], SPT is utilized to analyze the input-to-state multi-stable systems evolving on Riemannian manifolds. SPT is able to decompose the complex system into several order-reduced subsystems, which makes SPT a candidate solution to the control problem of nonaffine-in-control nonlinear systems. In [32], an SPT based control method, which is called ''approximate dynamic inversion'' (ADI), is developed for a class of nonaffine-in-control nonlinear systems to implement dynamic inversion. In order to derive the explicit inversion of each nonaffine functions, the authors in [32] establish a fast dynamic subsystem and guarantee the stability of the closed-loop system by SPT. In [33], ADI is utilized with backstepping to build controller for pure-feedback nonaffine-in-control nonlinear systems (PFNNSs). In [34], the authors employ ADI and parameter separation technique for nonlinearly parameterized pure-feedback systems. In [35], ADI is combined with a class of existing disturbance attenuation methods. It should be pointed out that the control input u evolves much faster than the other states in the ADI based schemes in [32]–[35]. This may lead to a high amplitude of actual input.

Motivated by the above facts, this paper proposes a novel FTDOs based ADI (FADI) control approach for PFNNSs with high-order mismatched disturbance and actuator saturation. With the outputs of FTDOs, the original system is reconstructed to form an equivalent saturated PFNNSs. In order to derive a controller for the nonaffine rebuilt system with actuator saturation, we modify the ADI design procedure with an extra intermediate subsystem. In the previous research on ADI [32]–[35], the controller is employed through a series of augmented dynamical equations to establish a boundary-layer subsystem (BLS). In our method, an additional intermediate subsystem is designed to compensate for the difference between the actual controller with and without actuator saturation. The entire system is separated into three subsystems, and the stability of the closed-loop system is guaranteed by Tikhonov's theorem.

The proposed scheme has the following features:

1) In [2], [11], [13], [15], the DOBC schemes only consider the affine-in-control nonlinear systems. In this paper, the FTDOs based control law can be applied to complete PFNNSs.

2) The ADI based controllers in [32]–[35] are developed without any input limitation. In this paper, we provide a modified ADI approach in the presence of actuator saturation, which makes the presented controller more practical.

3) In comparison with the traditional ADI methods in [32]–[35], the presented novel ADI design structure creates only one additional tuning parameter ε_1. This implies good feasibility from the perspective of application.

4) Both high-order mismatched disturbances and actuator saturation are considered for PFNNSs in this paper.

The paper is arranged as follows. Section II describes the problem formulation and presents some preliminaries on SPT. Section III provides the FADI controller design procedure. Section IV gives the main theorem and the stability proof. The simulation results are illustrated in Section V. Finally, some concluding remarks are given in Section VI.

II. PROBLEM FORMULATION AND PRELIMINARIES

A. PROBLEM FORMULATION

Consider the following PFNNSs with high-order mismatched disturbances and actuator saturation,

$$\begin{aligned} \dot{x}_i &= f_i(\bar{x}_i, x_{i+1}) + d_i, \\ \dot{x}_n &= f_n(\bar{x}_n, sat(u)) + d_n, \\ y &= x_1, \end{aligned} \tag{1}$$

where $i = 1, \ldots, n-1$, $\bar{x}_j = [x_1, x_2, \ldots, x_j]^T \in R^j$, and $u \in R$ are the states and control input, $j = 1, \ldots, n$. Also, d_n is the matched disturbance, d_i are the mismatched high-order disturbances enter the system via each channel with at least $(n-i)$th-order bounded derivatives, f_j are continuously

differentiable nonlinear functions in their arguments, and $sat(\cdot)$ is the saturation function defined as

$$sat(s) = sign(s) \cdot min\{M, |s|\}, \tag{2}$$

where M is a positive constant depending on the practical system. In this paper, we define the nominal system of (1) as

$$\begin{aligned} \dot{\bar{x}}_i &= f_i(\bar{x}_i, x_{i+1}), \\ \dot{\bar{x}}_n &= f_n(\bar{x}_n, u), \\ y &= x_1. \end{aligned} \tag{3}$$

Assumption 1: The reference signal y_r and its higher-order derivatives are available and bounded.

Assumption 2: For the nominal system in (3), $(\partial f_i/\partial x_{i+1})$ and $(\partial f_n/\partial u)$ are bounded away from zero for $\bar{x}_{i+1} \in \Omega_{\bar{x}_{i+1}} \subset D_{\bar{x}_{i+1}}$ and $(\bar{x}_n, u) \in \Omega_{\bar{x}_n,u} \subset D_{\bar{x}_n} \times D_u$, where $D_{\bar{x}_{i+1}} \subset R^{i+1}$, $D_{\bar{x}_n} \subset R^n$, $D_u \subset R$ are domains containing their respective origins, and $\Omega_{\bar{x}_{i+1}}$, $\Omega_{\bar{x}_n,u}$ are compact sets; that is $(\partial f_i/\partial x_{i+1})$ and $(\partial f_n/\partial u)$ are either positive or negative. Without losing the generality, we assume $(\partial f_i/\partial x_{i+1}) > 0$ and $(\partial f_n/\partial u) > 0$.

Remark 1: It is worth noting that this assumption is the standard context in which ADI is utilized [32]–[35].

The control objective is to develop a disturbance-observer-based method for the system in (1) to make $y \to y_r$ in any finite time interval despite the presence of high-order mismatched disturbances and actuator saturation.

B. PRELIMINARIES ON SINGULAR PERTURBATION THEORY

Consider the following nonlinear system [36],

$$\begin{aligned} \dot{x} &= f(t, x, z, \epsilon), \quad x(0) = \xi(\epsilon), \\ \epsilon\dot{z} &= g(t, x, z, \epsilon), \quad z(0) = \eta(\epsilon), \end{aligned} \tag{4}$$

where $0 < \epsilon \ll 1$ is small positive constant, $x \in R^n$ and $z \in R^m$, the functions $\xi(\epsilon)$ and $\eta(\epsilon)$ are smooth, the functions f and g are continuously differentiable in their arguments for $(t, x, z, \epsilon) \in [0, t_1] \times D_x \times D_z \times [0, \epsilon_0]$, where $t_1 \in (0, \infty)$, $D_x \subset R^n$ and $D_z \subset R^m$, $\epsilon_0 \gg 0$. The system described by (4) is in the 'standard singular perturbed form' (SSPF), if $0 = g(t, x, z, 0)$ has $k \geq 1$ isolated real roots $z = h_i(t, x)$, $i = 1, 2, \ldots, k$ for each $(t, x) \in [0, t_1] \times D_x$. For convenience we choose one fixed parameter $i \in 1, \ldots, k$, and drop the subscript i from h. Based on SPT [36], reduced-order subsystems can be obtained by substituting $\epsilon = 0$ in slow time-scale t and fast time-scale $\tau = \frac{t}{\epsilon}$. The 'reduced slow subsystem' (RSS) is described by

$$\dot{x} = f(t, x, h(t, x), 0), \quad x(0) = \xi_0, \tag{5}$$

and the 'boundary-layer subsystem' (BLS) is

$$\frac{dv}{d\tau} = g(t, x, v + h(t, x), 0), \quad v(0) = \eta_0 - h(0, \xi_0), \tag{6}$$

where $v = z - h(t, x)$, and $\xi_0 = \xi(0)$, $\eta_0 = \eta(0)$ are treated as fixed numbers.

Lemma 1 (Theorem 11.1 in [36]): Consider the singular perturbation problem of (4), and let $z = h(t, x)$ be an isolated root of $0 = g(t, x, z, 0)$. Assume that the following conditions are satisfied for all $(t, x, z - h(t, x), \epsilon) \in [0, t_1] \times D_x \times D_v \times [0, \epsilon_0]$ for $t_1 \in (0, \infty)$, and some domains $D_x \subset R^n$, $D_v \subset R^m$, which contain their respective origins.

(A1) The functions f, g, their first partial derivatives with respect to (x, z, ϵ), and the first partial derivative of g with respect to t are continuous; the function $h(t, x)$ and $[\partial g(t, x, z, 0)/\partial z]$ have continuous first partial derivatives with respect to their arguments; the initial data $\xi(\epsilon)$ and $\eta(\epsilon)$ are smooth functions of ϵ.

(A2) The reduced problem (5) has a unique solution $x_s(t) \in S$, for $t \in [t_0, t_1]$, where S is a compact subset of D_x.

(A3) The origin is an exponentially stable equilibrium point of the BLS (6), uniformly in (t, x). Let $R_v \subset D_v$ be the region of attraction of (6), and Ω_v be a compact subset of R_v.

Then there exists a positive constant $\epsilon^* > 0$, such that for all $t_0 \geq 0$, $\xi_0 \in \Omega_x$, $\eta_0 - h(t_0, \xi_0) \in \Omega_y$, and $0 < \epsilon \leq \epsilon^*$, the system (4) has a unique solution $x(t, \epsilon)$, $z(t, \epsilon)$ on $[t_0, t_1]$, and

$$\begin{aligned} x(t) &= x_s(t) + O(\varepsilon), \\ z(t) &= h(t, x_s) + v_f(t/\epsilon) + O(\varepsilon), \end{aligned} \tag{7}$$

hold uniformly for $t \in [t_0, t_1]$, where $O(\cdot)$ denotes the order of magnitude notation, and $v_f(\tau)$ is the solution of BLS (6).

Lemma 2 (Definition 11.1 in [36], Ch. 11): The equilibrium point $v = 0$ of the boundary-layer system (6) is exponentially stable, uniformly in $(t, x) \in [0, \infty) \times D_x$, if the Jacobian matrix $[\partial g/\partial v]$ satisfies the eigenvalue condition

$$\mathbf{Re}\left[\lambda\left\{\frac{\partial g}{\partial v}(t, x, h(t, x), 0)\right\}\right] \leq -c < 0, \tag{8}$$

for all $(t, x) \in [0, \infty) \times D_x$.

Lemma 1 has been known as the Tikhonov's theorem. It reveals that important stability information about the full singularly perturbed system can be obtained by studying the RSS and the BLS through the approximation in (7) in any finite time interval.

III. CONTROLLER DESIGN

A. FTDOs AND MODEL RECONSTRUCTION

Since the effect of the mismatched disturbances cannot be eliminated completely from the state variables [11], we first reconstruct the PFNNSs in (1) with the outputs of the FTDOs.

Inspired by [2], [11], [13], we employ FTDOs to estimate the disturbances as well as their time derivatives,

$$\begin{aligned} \dot{z}_0^i &= v_0^i + f_i(\bar{x}_i, x_{i+1}), \\ v_0^i &= -\lambda_{i0}|z_0^i - x_i|^{\frac{r_i}{r_i+1}} sign(z_0^i - x_i) + z_1^i, \\ \dot{z}_j^i &= v_j^i, \\ v_j^i &= -\lambda_{ij}|z_j^i - v_{j-1}^i|^{\frac{r_i-j}{r_i-j+1}} sign(z_j^i - v_{j-1}^i) + z_{j+1}^i, \end{aligned} \tag{9}$$

where z_0^i are the estimates of states x_i, z_j^i $(j = 1, \ldots, r_i; i = 1, \ldots, n-1)$ are the estimates of the disturbances and their derivatives $d_i^{(j-1)}$. The superscript '$(j-1)$' represents the $(j-1)$th-order derivative of the variable with respect to t. Also,

$r_i = n - i + 1$ represent the orders of FTDOs, $z^i_{r_i+1} = 0$, and $\lambda_{ij} = \lambda^i_j L_i^{(\frac{1}{r_i-j+1})}$ are the designed parameters of the observers, $\lambda^i_j > 0$ are some positive designed coefficients, L_i are the Lipschitz constants of $d_i^{(r_i)}$.

The estimate errors are defined as $e^i_0 = z^i_0 - x_i$, $e^i_j = z^i_j - d_i^{(j-1)}$, $e^i_j = z^n_j - d_n^{(j-1)}$, $e^i_{r_i+1} = 0$. The error dynamics of FTDOs are derived as in [11],

$$\begin{aligned}\dot{e}^i_0 &= -\lambda_{i0}|e^i_0|^{\frac{r_i}{r_i+1}} sign(e^i_0) + e^i_1,\\ \dot{e}^i_j &= -\lambda_{ij}|e^i_j - \dot{e}^i_{j-1}|^{\frac{r_i-j}{r_i-j+1}} sign(e^i_j - \dot{e}^i_{j-1}) + e^i_{j+1}.\end{aligned} \quad (10)$$

As in [11], [13], the estimate errors $e^i_j(t)$ will converge to the origin in finite time. This implies that there is a time constant $t_f > 0$ such that $e^i_j(t) = 0$ for all $t > t_f$. Moreover, after a finite time of t_f, the following equality is true: $z^i_j = v^i_{j-1}$.

Remark 2: The parameters of λ_{ij} can be chosen according to [13], [14]. The observer gains should be assigned large values to ensure a fast convergence of the estimation error. However, this may introduce high frequency noise and degrade the tracking performance. Thus, designers have to compromise between these aspects to achieve a satisfactory performance.

The system in (1) can be reconstructed with the outputs of the FTDOs in (9). Define new states as $\hat{x}_1 = x_1, \hat{x}_2 = x_2 + z^1_1$, $\hat{x}_3 = x_3 + z^1_2 + z^2_1, \ldots, \hat{x}_{n-1} = x_{n-1} + z^1_{n-2} + z^2_{n-3} + \cdots + z^{n-2}_1$ and $\hat{x}_n = x_n + z^1_{n-1} + z^2_{n-2} + \cdots + z^{n-1}_1$. The system in (1) is represented as the following equivalent system,

$$\begin{aligned}\dot{\hat{x}}_1 &= f_1(x_1, x_2) + d_1\\ &= \left[f_1(x_1, x_2) + z^1_1\right] + (d_1 - z^1_1)\\ &= \hat{f}_1(\hat{x}_1, \hat{x}_2, z^1_1) + (d_1 - z^1_1)\\ &= \hat{f}_1(\hat{x}_1, \hat{x}_2, z^1_1) - e^1_1,\\ \dot{\hat{x}}_2 &= f_2(\bar{x}_2, x_3) + d_2 + v^1_1\\ &= \left[f_2(\bar{x}_2, x_3) + z^1_2 + z^2_1\right] + \left[(v^1_1 - z^1_2) + (d_2 - z^2_1)\right]\\ &= \hat{f}_2(\bar{\hat{x}}_2, \hat{x}_3, z^1_1, z^1_2, z^2_1) + \left[(\dot{e}^1_1 - e^1_2) - e^2_1\right],\\ &\vdots\\ \dot{\hat{x}}_i &= \hat{f}_i(\bar{\hat{x}}_i, \hat{x}_{i+1}, \bar{z}_i) + [(\dot{e}^1_{i-1} - e^1_i) + (\dot{e}^2_{i-2} - e^2_{i-1}) +\\ &\quad \cdots + (\dot{e}^{i-1}_1 - e^{i^1}_2) - e^i_1],\\ &\vdots\\ \dot{\hat{x}}_n &= \hat{f}_n(\bar{\hat{x}}_n, sat(u), \bar{z}_n) + \left[(\dot{e}^1_{n-1} - e^1_n) + \ldots - e^n_1\right],\end{aligned} \quad (11)$$

where $\bar{\hat{x}}_j = [\hat{x}_1, \ldots, \hat{x}_j]^T$ and $\bar{z}_j = [z^1_1, \ldots, z^1_j, z^2_1, \ldots, z^j_1]^T$ are vectors of appropriate dimensions, $j = 1, \ldots, n$. Rewrite (11) as the following compact form,

$$\dot{\hat{x}} = \hat{f}(\bar{\hat{x}}_n, sat(u), \bar{z}_n) + \hat{e}, \quad (12)$$

where $\hat{e} = [\hat{e}_1, \ldots, \hat{e}_n]^T \in R^n$ is the estimate error vector. The components of $\hat{e}$ are defined by $\hat{e}_1 = -e^1_1$, $\hat{e}_2 = (\dot{e}^1_1 - e^1_2) - e^2_1, \ldots, \hat{e}_n = (\dot{e}^1_{n-1} - e^1_n) + \cdots - e^n_1$.

B. MODIFIED ADI CONTROLLER DESIGN

Consider the nominal system of (12)

$$\dot{\hat{x}} = \hat{f}(\bar{\hat{x}}_n, u, \bar{z}_n). \quad (13)$$

The controller is designed in n steps. The first $n-1$ steps are the same as the ADI based backstepping controller design procedure in [33]–[35]. In the last step, an extra variable ω is introduced and an augmented intermediate subsystem is built to attenuate the effect of the actuator saturation.

Step 1. Consider the first equation in (13),

$$\dot{\hat{x}}_1 = \hat{f}_1(\hat{x}_1, \hat{x}_2, \bar{z}_1). \quad (14)$$

Substituting $e_1 = \hat{x}_1 - \alpha_0 = x_1 - y_r$, we have

$$\dot{e}_1 = \hat{f}_1(\hat{x}_1, \hat{x}_2, \bar{z}_1) - \dot{\alpha}_0. \quad (15)$$

We consider $\hat{x}_2$ as a control variable according to backstepping design procedure. Then the virtual controller is defined as $\alpha_1 = \hat{x}_2 - e_2$, and its dynamic is designed as

$$\varepsilon\dot{\alpha}_1 = -sign\left(\frac{\partial Q_1}{\partial \alpha_1}\right) Q_1, \quad (16)$$

where $\varepsilon > 0$ is a designed singular perturbation parameter, and Q_1 is a function defined as

$$Q_1(\bar{e}_2, \alpha_1, \bar{z}_1) = k_1 e_1 + \hat{f}_1(\hat{x}_1, e_2 + \alpha_1, \bar{z}_1) - \dot{\alpha}_0, \quad (17)$$

where $k_1 > 0$ is a positive feedback gain, $\bar{e}_2 = [e_1, e_2]^T \in R^2$. Let $h_1(\bar{e}_2, \bar{z}_1)$ be an isolated root of $Q_1(\bar{e}_2, \alpha_1, \bar{z}_1) = 0$, the system in (15) and (16) can be written in the SSPF,

$$\begin{aligned}\dot{e}_1 &= \hat{f}_1(\hat{x}_1, e_2 + (y_1 + h_1), \bar{z}_1) - \dot{\alpha}_0,\\ \varepsilon\dot{y}_1 &= -sign\left(\frac{\partial Q_1}{\partial \alpha_1}\right) Q_1 - \varepsilon\dot{h}_1,\end{aligned} \quad (18)$$

where $y_1 = \alpha_1 - h_1$. Based on SPT, as $\varepsilon \to 0$, the BLS of (18) can be derived as

$$\frac{dy_1}{d\tau} = -sign\left(\frac{\partial Q_1}{\partial \alpha_1}\right) Q_1, \quad (19)$$

and the corresponding RSS of (18) is

$$\dot{e}_1 = \hat{f}_1(\hat{x}_1, e_2 + h_1, \bar{z}_1) - \dot{\alpha}_0 = -k_1 e_1, \quad (20)$$

where $\tau = \frac{t}{\varepsilon}$. It can be seen that the fast state α_1 will be driven to the desired manifold h_1, which works as a pseudo controller and stabilizes RSS.

Step i. Repeat the aforementioned procedure, and rewrite the ith equation in (13) with $e_i = \hat{x}_i - \alpha_{i-1}$,

$$\dot{e}_i = \hat{f}_i(\bar{\hat{x}}_i, \hat{x}_{i+1}, \bar{z}_i) - \dot{\alpha}_{i-1}. \quad (21)$$

Consider $\hat{x}_{i+1}$ as the control variable, the virtual controller is defined as $\alpha_i = \hat{x}_{i+1} - e_{i+1}$. The dynamic of α_i is written as

$$\varepsilon\dot{\alpha}_i = -sign\left(\frac{\partial Q_i}{\partial \alpha_i}\right) Q_i, \quad (22)$$

where Q_i is a function defined as

$$Q_i(\bar{e}_{i+1}, \alpha_i, \bar{z}_i) = k_i e_i + \hat{f}_i(\bar{\hat{x}}_i, e_{i+1} + \alpha_i, \bar{z}_i) - \dot{\alpha}_{i-1}, \quad (23)$$

where $k_i > 0$ is the positive feedback gain, $\bar{e}_{i+1} = [e_1, \ldots, e_{i+1}]^T \in R^{i+1}$. Let $h_i(\bar{e}_{i+1}, \bar{z}_i)$ be an isolated root of $Q_i(\bar{e}_{i+1}, \alpha_i, \bar{z}_i) = 0$, the system in (21) and (22) can be written in SSPF,

$$\begin{aligned} \dot{e}_i &= \hat{f}_i(\bar{\hat{x}}_i, e_{i+1} + (y_i + h_i), \bar{z}_i) - \dot{\alpha}_{i-1}, \\ \varepsilon \dot{y}_i &= -sign\left(\frac{\partial Q_i}{\partial \alpha_i}\right) Q_i - \varepsilon \dot{h}_i, \end{aligned} \tag{24}$$

where $y_i = \alpha_i - h_i$. As $\varepsilon \to 0$, the corresponding BLS and RSS can be deduced as

$$\frac{dy_i}{d\tau} = -sign\left(\frac{\partial Q_i}{\partial \alpha_i}\right) Q_i, \tag{25}$$

and

$$\dot{e}_i = \hat{f}_i(\bar{\hat{x}}_i, e_{i+1} + h_i, \bar{z}_i) - \dot{\alpha}_{i-1} = -k_i e_i. \tag{26}$$

Remark 3: It can be seen that the time derivative of virtual control input in the ith step, as $\dot{\alpha}_i$ in (22), is already calculated in the $(i-1)$th step. Therefore the problem of 'explosion of complexity' in backstepping design is avoided.

Step n. In the nth step, the dynamic of the actual control input u can be designed as

$$\varepsilon \dot{u} = -sign\left(\frac{\partial Q_n}{\partial u}\right) Q_n, \tag{27}$$

where Q_n is a function defined as

$$Q_n(\bar{e}_n, u, \bar{z}_n, \omega) = k_n e_n + \hat{f}_n(\bar{\hat{x}}_n, u, \bar{z}_n) - \dot{\alpha}_{n-1} + \omega, \tag{28}$$

where $\hat{f}_n$ is the nth element of $\hat{f}$ in (13), $k_n > 0$ is the nth positive feedback gain, $\bar{e}_n = [e_1, \ldots, e_n]^T \in R^n$, $e_n = \hat{x}_n - \alpha_{n-1}$, and ω will be defined later.

Now we add actuator saturation to the nominal system. Then the nth equation under actuator saturation can be expressed in the error coordinate as

$$\begin{aligned} \dot{e}_n &= \hat{f}_n(\bar{\hat{x}}_n, sat(u), \bar{z}_n) - \dot{\alpha}_{n-1} - \varepsilon \dot{h}_n \\ &\quad + \hat{f}_n(\bar{\hat{x}}_n, u, \bar{z}_n) - \hat{f}_n(\bar{\hat{x}}_n, u, \bar{z}_n) \\ &= \hat{f}_n(\bar{\hat{x}}_n, u, \bar{z}_n) - \dot{\alpha}_{n-1} - \varepsilon \dot{h}_n \\ &\quad + \left[\hat{f}_n(\bar{\hat{x}}_n, sat(u), \bar{z}_n) - \hat{f}_n(\bar{\hat{x}}_n, u, \bar{z}_n)\right], \end{aligned} \tag{29}$$

where $y_n = u - h_n$.

Then, we design ω to compensate $[\hat{f}_n(\bar{\hat{x}}_n, sat(u), \bar{z}_n) - \hat{f}_n(\bar{\hat{x}}_n, u, \bar{z}_n)]$ in (29),

$$\varepsilon_1 \dot{\omega} = -sign\left(\frac{\partial Q_\omega}{\partial \omega}\right) Q_\omega, \tag{30}$$

where ε_1 is a designed parameter satisfying

$$0 < \varepsilon \ll \varepsilon_1 \ll 1, \tag{31}$$

and Q_ω is a function designed as

$$Q_\omega(\bar{e}_n, u, \bar{z}_n, \omega) = \hat{f}_n(\bar{\hat{x}}_n, sat(u), \bar{z}_n) - \hat{f}_n(\bar{\hat{x}}_n, u, \bar{z}_n) - \omega. \tag{32}$$

This completes the controller design procedure.

IV. STABILITY ANALYSIS

The main result of this work can be summarized from the following theorem.

Theorem 1: Consider the PFNNSs in (1) with high-order mismatched disturbances and actuator saturation. The nominal system in (3) satisfies Assumptions 1 and 2. Let $h_n(\bar{e}_n, \bar{z}_n, \omega)$ and $h_\omega(\bar{e}_n, u, \bar{z}_n)$ be the isolated roots of $Q_n(\bar{e}_n, u, \bar{z}_n, \omega) = 0$ and $Q_\omega(\bar{e}_n, u, \bar{z}_n, \omega) = 0$. Assuming the following conditions hold for all $[\bar{e}_{j+1}, y_j, y_\omega] \in D_{\bar{e}_{j+1}} \times D_{y_j} \times D_{y_\omega}$ for some domains $D_{\bar{e}_{j+1}} \subset R^{j+1}$, $D_{y_j} \subset R$, and $D_{y_\omega} \subset R$ which contain their respective origins, where $y_n = u - h_n$, $y_\omega = \omega - h_\omega$, $\bar{e}_{n+1} = \bar{e}_n$, $D_{\bar{e}_{n+1}} = D_{\bar{e}_n}$, $\alpha_n = u$, $j = 1, \ldots, n$.

(B1) The functions Q_j, Q_ω, $\dot{h}_j$, $\dot{h}_\omega$, and their first partial derivatives with respect to their arguments and t are continuous; h_j, h_ω, $[\partial Q_j/\partial \alpha_j]$, $[\partial Q_\omega/\partial \omega]$ have continuous first partial derivatives with respect to their arguments.

(B2) $(\bar{e}_{j+1}, y_j) \mapsto (\partial Q_j/\partial \alpha_j)$ and $(\bar{e}_n, y_\omega) \mapsto (\partial Q_\omega/\partial \omega)$ are bounded below by some positive constant for all $\bar{e}_{j+1} \in D_{\bar{e}_{j+1}}$.

Then, under the controller designed by (16), (22), (27), and (30) with the FTDOs in (9), there exists two tuning parameters ε, ε_1 such that the system output y will track the desired signal y_r, and the error states $\bar{e}_n$ will remain bounded uniformly for any finite time interval in spite of the presence of high-order mismatched disturbances and actuator saturation.

Proof: Under the controller in (16), (22), (27) and (30), the reconstructed PFNNSs in (11) can be written in the closed-loop form in error coordinate,

$$\begin{aligned} \dot{e}_1 &= \hat{f}_1(\hat{x}_1, e_2 + (y_1 + h_1), \bar{z}_1) - \dot{\alpha}_0 + \hat{e}_1, \\ &\vdots \\ \dot{e}_i &= \hat{f}_i(\bar{\hat{x}}_i, e_{i+1} + (y_i + h_i), \bar{z}_i) - \dot{\alpha}_{i-1} + \hat{e}_i, \\ &\vdots \\ \dot{e}_n &= \hat{f}_n(\bar{\hat{x}}_n, y_n + h_n, \bar{z}_n) + [\hat{f}_n(\bar{\hat{x}}_n, sat(y_n + h_n), \bar{z}_n) \\ &\quad - \hat{f}_n(\bar{\hat{x}}_n, y_n + h_n, \bar{z}_n)] - \dot{\alpha}_{n-1} + \hat{e}_n, \\ \varepsilon_1 \dot{y}_\omega &= -sign\left(\frac{\partial Q_\omega}{\partial \omega}\right) Q_\omega - \varepsilon_1 \dot{h}_\omega, \\ \varepsilon \dot{\mathbf{y}} &= \Gamma q - \varepsilon \dot{h}, \end{aligned} \tag{33}$$

where $\mathbf{y} = [y_1, \ldots, y_n]^T \in R^n$, $h = [h_1, h_2, \ldots, h_n]^T \in R^n$, $q = [Q_1, Q_2, \ldots, Q_n]^T$, and

$$\Gamma = \begin{bmatrix} -sign\left(\frac{\partial Q_1}{\partial \alpha_1}\right) & & \\ & \ddots & \\ & & -sign\left(\frac{\partial Q_n}{\partial u}\right) \end{bmatrix}. \tag{34}$$

As $\varepsilon \to 0$, the BLS and the RSS of (33) can be derived as

$$\frac{d\mathbf{y}}{d\tau} = \Gamma q, \tag{35}$$

and

$$\begin{aligned}\dot{e}_i &= -k_i e_i + \hat{e}_i,\\ \dot{e}_n &= -k_n e_n + \hat{f}_n(\bar{\hat{x}}_n, sat(h_n), \bar{z}_n) - \hat{f}_n(\bar{\hat{x}}_n, h_n, \bar{z}_n)\\ &\quad - \omega + \hat{e}_n,\\ \varepsilon_1 \dot{y}_\omega &= -sign\left(\frac{\partial Q_\omega}{\partial \omega}\right) Q_\omega - \varepsilon_1 \dot{h}_\omega. \end{aligned} \tag{36}$$

Follow [32]–[35], the local exponential stability of BLS in (35) is achieved with Lemma 2, Assumption 2 and (B2), since

$$sign\left(\frac{\partial Q_i}{\partial \alpha_i}\right) > 0, \tag{37}$$

$$sign\left(\frac{\partial Q_n}{\partial u}\right) > 0. \tag{38}$$

This suggests that we can use RSS in (36) to approximate the closed-loop system in (33) based on Tikhonov's theorem and (7). Thus, we have

$$\bar{e}_n = \bar{e}_s + O(\varepsilon), \tag{39}$$

where $\bar{e}_s \in R^n$ denotes the solution vector of RSS in (36). Observe that RSS in (36) is in SSPF. Meanwhile, ω evolves slower than u, which is treated as a fixed point h_n in (36). We can use ω to compensate the perturbation term $[\hat{f}_n(\bar{\hat{x}}_n, sat(h_n), \bar{z}_n) - \hat{f}_n(\bar{\hat{x}}_n, h_n, \bar{z}_n)]$ in RSS. The relatively fast and slow subsystem of (36) can be derived, respectively, as $\varepsilon_1 \to 0$,

$$\frac{dy_\omega}{d\tau_1} = -sign\left(\frac{\partial Q_\omega}{\partial \omega}\right) Q_\omega, \tag{40}$$

and

$$\dot{\bar{e}}_{ss} = A\bar{e}_{ss} + \hat{e}, \tag{41}$$

where $\bar{e}_{ss} \in R^n$ represents the solution vector of relatively slow subsystem (41), $\tau_1 = \frac{t}{\varepsilon_1}$, and $A = diag(-k_1, -k_2, -k_3, \ldots, -k_n)$ is a Hurwitz matrix.

Linearize (40) at the equilibrium $y_\omega = 0$, the corresponding eigenvalue is $\lambda_\omega = -1$. Thus the local exponential stability of (40) can also be obtained with Lemma 2. Therefore, we can use the relatively slow subsystem in (41) to approximate RSS in (36).

As in [11], a finite-time bounded (FTB) function can be defined for (41) as

$$V(\bar{e}_{ss}) = \frac{1}{2}\bar{e}_{ss}^T \bar{e}_{ss}. \tag{42}$$

Differentiate (42) along the trajectory of (41),

$$\begin{aligned}\dot{V}(\bar{e}_{ss}) &= \bar{e}_{ss}^T A\bar{e}_{ss} + \bar{e}_{ss}^T \hat{e}\\ &\le \bar{e}_{ss}^T A\bar{e}_{ss} + \frac{1}{2}(\bar{e}_{ss}^T \bar{e}_{ss} + \hat{e}^T \hat{e})\\ &\le \left(\lambda_{max}(A) + \frac{1}{2}\right)\bar{e}_{ss}^T \bar{e}_{ss} + \frac{1}{2}\left\|\hat{e}\right\|^2, \end{aligned} \tag{43}$$

where $\lambda_{max}(A)$ denotes the largest eigenvalue of A. Since A is Hurwitz, it follows from [11] that once the finite-time stability of FTDOs in (9) is obtained in finite time, the output y_{ss} of the relatively slow subsystem in (41) will be driven to y_r asymptotically and the error states $\bar{e}_{ss}$ will remain bounded.

Based on the Tikhonov's theorem and (7), the output of closed-loop system can be approximated in any finite time interval by the output of the relatively slow subsystem,

$$y(t) = y_{ss}(t) + O(\varepsilon) + O(\varepsilon_1), \tag{44}$$

which can be shorten as

$$y(t) = y_{ss}(t) + O(\varepsilon_1), \tag{45}$$

since $\varepsilon \ll \varepsilon_1$.

It can then be concluded that the output y will track the desired signal y_r in any finite time interval and the error states $\bar{e}_n = [e_1, \ldots, e_n]^T$ will remain bounded despite the presence of the high-order mismatched disturbances and actuator saturation. □

Remark 4: The closed-loop system is approximated by the relatively slow subsystem. Thus the feedback gains of FTDOs are related with tracking and stability performance. It is known that the FTDOs can achieve finite time fast convergence property, whose dynamics can be designed much faster than the dynamics of the asymptotic disturbance observer [11]. Thus, the FTDOs gains should be assigned large enough to achieve fast convergence. However, the values of the gains of FTDOs can not be too large to avoid resulting in an excessive transient peaking.

Remark 5: The singular perturbation parameters ε, ε_1 should be tuned to ensure the effectiveness of the time-scale split of the closed-loop system, which indicates that they should be assigned to satisfy (31). Meanwhile, both ε and ε_1 should be small enough to ensure that BLS and the relatively fast subsystem evolve faster than the FTDOs, which work in the relatively slow subsystem.

Remark 6: The proposed control law is specific to single-input-single-output systems, so multi-input-multi-output (MIMO) systems are not considered in this paper. For MIMO nonaffine-in-control nonlinear systems with high-order mismatched disturbances and input saturation, some topics should be further investigated. For instance, the structure of the MIMO nominal system, the form of the controller and observers, the stability of the closed-loop system, etc., should all be taken into account.

V. SIMULATION

In order to demonstrate the effectiveness of the proposed control method, two simulation examples are presented. In the first example, a second order PFNNSs in [34] is utilized to validate the stabilization performance of the proposed scheme. In the second example, we apply FADI control law to a real world application system in [37], [38]. To highlight the merits of the FADI control approach, the ADI based backstepping (ABB) controller in [33], [34] is applied to both examples without actuator saturation.

A. NUMERICAL EXAMPLE

Consider the following system in [34],

$$\begin{aligned}\dot{x}_1 &= 0.4x_2 + \frac{x_2^3}{2} + ln\left(1+(\gamma_1 x_1)^2\right) + d_1,\\ \dot{x}_2 &= x_2^2 sat(u) + tanh\left(sat(u)\right) + \frac{\gamma_2 x_1^2}{(1+\gamma_1 x_2)^2 + x_2^2} + d_2,\\ y &= x_1,\end{aligned} \tag{46}$$

where $\gamma_1 = 2.5$, $\gamma_2 = 1.6$, the disturbances are $d_1 = 15 + x_1 + \sin(5t)$, $d_2 = 3 + 5\sin(5t)$, and the input limitation is $M = 10$. To implement the FADI method, the FTDOs can be designed as

$$\begin{aligned}\dot{z}_0^1 &= v_0^1 + \left(0.4x_2 + \frac{x_2^3}{2} + ln\left(1+(\gamma_1 x_1)^2\right)\right),\\ v_0^1 &= -\lambda_{10}|z_0^1 - x_1|^{\frac{2}{3}} sign(z_0^1 - x_1) + z_1^1,\\ \dot{z}_1^1 &= v_1^1,\\ v_1^1 &= -\lambda_{11}|z_1^1 - v_0^1|^{\frac{1}{2}} sign(z_1^1 - v_0^1) + z_2^1,\\ \dot{z}_2^1 &= v_2^1,\\ v_2^1 &= -\lambda_{12} sign(z_2^1 - v_1^1),\\ \dot{z}_0^2 &= v_0^2 + \left(x_2^2 sat(u) + tanh(sat(u)) + \frac{\gamma_2 x_1^2}{(1+\gamma_1 x_2)^2 + x_2^2}\right),\\ v_0^2 &= -\lambda_{20}|z_0^2 - x_2|^{\frac{1}{2}} sign(z_0^2 - x_2) + z_1^2,\\ \dot{z}_1^2 &= v_1^2,\\ v_1^2 &= -\lambda_{21} sign(z_1^2 - v_0^2),\end{aligned} \tag{47}$$

where z_0^1 and z_0^2 are the estimates of x_1 and x_2, z_1^1 and z_1^2 are the estimates of d_1 and d_2, z_2^1 is the estimate of $\dot{d}_1$. With the outputs of FTDOs (47), the system in (46) can be reconstructed as

$$\begin{aligned}\dot{\hat{x}}_1 &= \hat{f}_1(\bar{\hat{x}}_2, \bar{z}_1) + \hat{e}_1\\ &= 0.4(\hat{x}_2 - z_1^1) + \frac{(\hat{x}_2 - z_1^1)^3}{2} + ln\left(1+(\gamma_1 \hat{x}_1)^2\right)\\ &\quad + z_1^1 + \hat{e}_1,\\ \dot{\hat{x}}_2 &= \hat{f}_2(\bar{\hat{x}}_2, sat(u), \bar{z}_2) + \hat{e}_2\\ &= (\hat{x}_2 - z_1^1)^2 sat(u) + tanh(sat(u))\\ &\quad + \frac{\gamma_2 \hat{x}_1^2}{(1+\gamma_1 \hat{x}_2 - \gamma_1 z_1^1)^2 + x_2^2} + z_2^1 + z_1^2 + \hat{e}_2.\end{aligned} \tag{48}$$

Then the controllers can be designed as

$$\begin{aligned}Q_1 &= k_1 e_1 + \hat{f}_1(\bar{\hat{x}}_2, z_1^1) - \dot{y}_r,\\ Q_2 &= k_2 e_2 + \hat{f}_2(\bar{\hat{x}}_2, u, \bar{z}_2) - \dot{\alpha}_1 + \omega,\\ Q_\omega &= \hat{f}_2(\bar{\hat{x}}_2, sat(u), \bar{z}_2) - \hat{f}_2(\bar{\hat{x}}_2, u, \bar{z}_2) - \omega,\\ \varepsilon\dot{\alpha}_1 &= -sign\left(\frac{\partial Q_1}{\partial \alpha_1}\right) Q_1,\\ \varepsilon\dot{u} &= -sign\left(\frac{\partial Q_2}{\partial u}\right) Q_2,\\ \varepsilon_1\dot{\omega} &= -sign\left(\frac{\partial Q_\omega}{\partial \omega}\right) Q_\omega.\end{aligned} \tag{49}$$

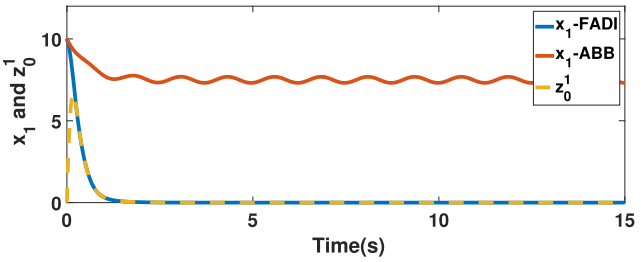

FIGURE 1. Trajectories of x_1 and z_0^1.

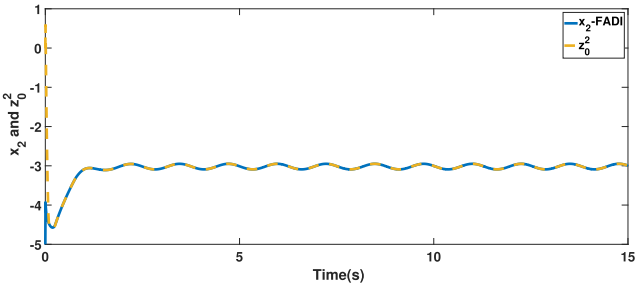

FIGURE 2. Trajectories of x_2 and its estimate z_0^2.

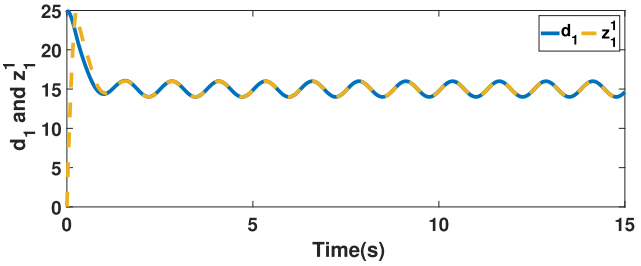

FIGURE 3. Trajectories of d_1 and its estimate z_1^1.

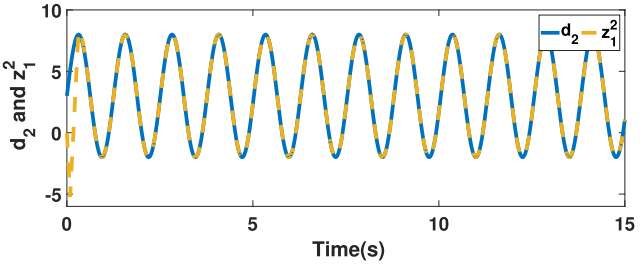

FIGURE 4. Trajectories of d_2 and its estimate z_1^2.

The initial conditions are set as $x_1(0) = 10$, $x_2(0) = -5$, $u(0) = 0$, the reference signal is $y_r = 0$. As mentioned in the Remark 4, the gains of the FTDOs are $\lambda_{10} = 10 \times 15^{\frac{1}{3}}$, $\lambda_{11} = 4 \times 15^{\frac{1}{2}}$, $\lambda_{12} = 4 \times 15$, $\lambda_{20} = 10 \times 15^{\frac{1}{2}}$, $\lambda_{21} = 2 \times 15$. The feedback gains of the controllers are chosen as $k_1 = 2$, $k_2 = 3$, and the singular perturbation parameters are $\varepsilon = 0.001$, $\varepsilon_1 = 0.01$.

As shown in Fig. 1, the output of the system under FADI converges to the origin within 1 second. By comparison, the ABB controller causes large tracking error and makes the output vibrate permanently in the presence of high-order mismatched disturbances. Fig. 1 - Fig. 4 depict that the FTDOs

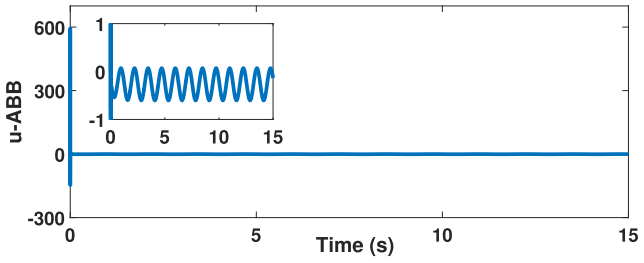

FIGURE 5. Time response of ABB controller without actuator saturation.

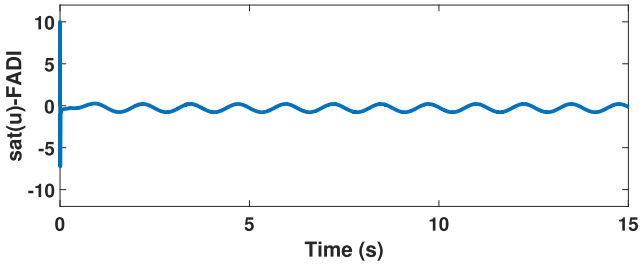

FIGURE 6. Time response of FADI controller with actuator saturation.

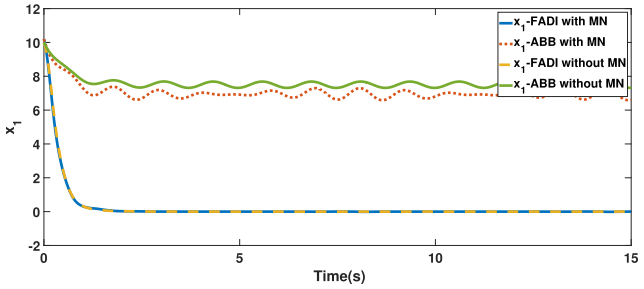

FIGURE 7. Trajectories of x_1 with and without MN.

estimate the states and disturbances accurately and timely for the nonaffine-in-control nonlinear system in (46). This validates that the application scope of FTDOs is extended by the proposed control law. As can be observed in Fig. 5 - Fig. 6, the amplitude of ABB controller is almost 600, whereas the actual input of FADI controller is restricted within the desired region. This implies that the presented modified ADI control technique successfully attenuates the influence of actuator saturation.

To further illustrate the performance of the presented scheme, we assume the states of (46) are also corrupted by the measurement noises (MN): $d_{1m} = 0.2 + 0.1\sin t$ and $d_{2m} = 0.1\cos^2 3t$. For comparison, other conditions and parameters are the same.

Fig. 7 and Fig. 8 present the evolutions of states of the system (46) under both controllers. Observe that the FADI controller retains perfect stabilization performance despite the erroneous MN. In contrast, the trajectories of the states under ABB controller are obviously affected by MN. Fig. 9 demonstrates that the input signal of FADI remains in the designated region.

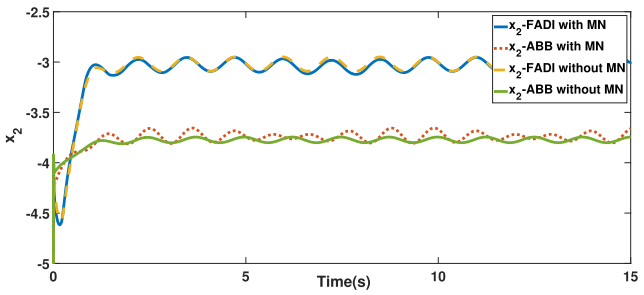

FIGURE 8. Trajectories of x_2 with and without MN.

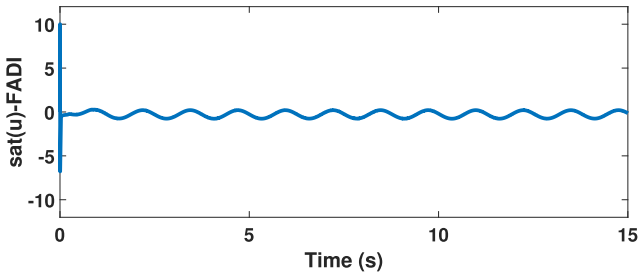

FIGURE 9. Time response of input of FADI with MN.

B. ONE-DOF LINK MANIPULATOR WITH BDC MOTOR

Consider the following one-link robotic system with a brush DC (BDC) motor in [37], [38],

$$\begin{aligned} D\ddot{\theta} + B\dot{\theta} + N\sin(\theta) &= \tau_B, \\ L\dot{\tau}_B + H\tau_B + K_m\dot{\theta} &= V, \end{aligned} \tag{50}$$

where $D = \frac{J}{K_\tau} + \frac{mL_0^2}{3K_\tau} + \frac{M_0^2}{K_\tau} + \frac{2M_0R_0^2}{5K_\tau}$, $N = \frac{mL_0^2G}{2K_\tau} + \frac{M_0L_0G}{K_\tau}$, and $B = \frac{B_0}{K_\tau}$. The physical parameters of one-DOF link manipulator with BDC motor are $J = 1.625 \times 10^{-3}$ kg$\cdot$ m^2, $m = 1$kg, $R_0 = 0.023$ m, $M_0 = 0.434$ kg, $L_0 = 0.305$ m, $B_0 = 16.25 \times 10^{-3}$ N$\cdot$m$\cdot$s/rad, $L = 25.0 \times 10^{-3}$ H, $G = 9.8$ m/s^2, $H = 5.0\ \Omega$, and $K_\tau = K_m = 0.9$ N$\cdot$m/A. Let $x_1 = \theta$, $x_2 = \dot{\theta}$, $x_3 = \tau_B$, $u = V$.

Then the system in (50) with high-order mismatched disturbances and actuator saturation can be written as

$$\begin{aligned} \dot{x}_1 &= f_1(x_1, x_2) + d_1, \\ \dot{x}_2 &= f_2(\bar{x}_2, x_3) + d_2, \\ \dot{x}_3 &= f_3(\bar{x}_3, sat(u)) + d_3, \\ y &= x_1, \end{aligned} \tag{51}$$

where $f_1(x_1, x_2) = x_2$, $f_2(\bar{x}_2, x_3) = -\frac{Bx_2}{D} - \frac{N\sin x_1}{D} + \frac{x_3}{D}$, $f_3(\bar{x}_3, u) = \frac{-K_m x_2}{L} - \frac{Hx_3}{L} + \frac{u}{L}$. In this example, a time-varying reference trajectory described as $y_r = 1 + \sin\frac{\pi}{2}t$ is designated for the system (51) to track. The high-order mismatched disturbances are $d_1 = 1 + 0.2\sin(2t) + x_1$, $d_2 = 3 + 0.1\cos t$, $d_3 = 0.5\cos 35t$. The input constraint is $M = 10$. The initial conditions are $x_1(0) = 0$, $x_2(0) = 2$, $x_3(0) = 1$, $u(0) = 0$. The parameters of FTDOs are chosen as $\lambda_{10} = 20\times30^{\frac{1}{4}}, \lambda_{11} = 10\times30^{\frac{1}{3}}, \lambda_{12} = 5\times30^{\frac{1}{2}}, \lambda_{13} = 3\times30$, $\lambda_{20} = 10\times30^{\frac{1}{3}}, \lambda_{21} = 1\times30^{\frac{1}{2}}, \lambda_{22} = 1\times30, \lambda_{30} = 10\times30^{\frac{1}{2}}$,

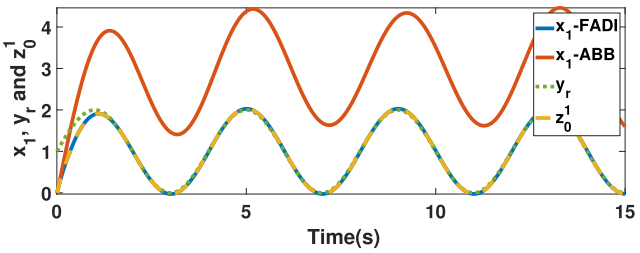

FIGURE 10. Trajectories of x_1, y_r, and z_0^1.

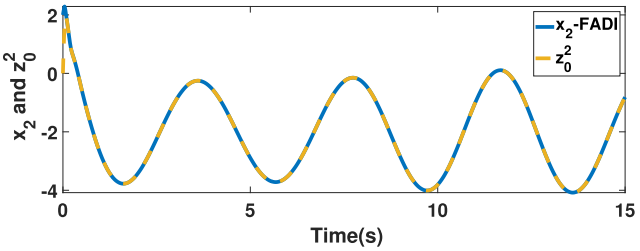

FIGURE 11. Trajectories of x_2 and its estimate z_0^2.

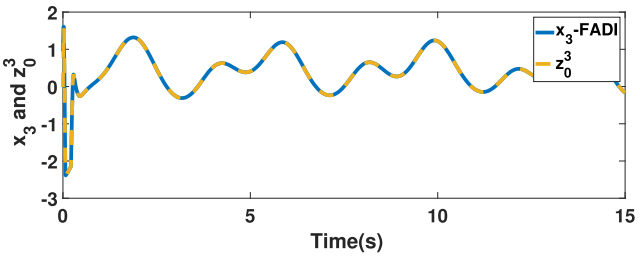

FIGURE 12. Trajectories of x_3 and its estimate z_0^3.

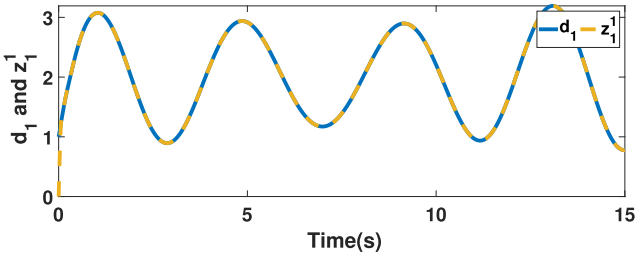

FIGURE 13. Trajectories of d_1 and its estimate z_1^1.

$\lambda_{31} = 0.5 \times 30$. The feedback gains of both controllers are set as $k_1 = 1$, $k_2 = 3$, $k_3 = 5$. The singular perturbation parameters are $\varepsilon = 1/30$, $\varepsilon_1 = 0.1$.

Fig. 10 - Fig. 16 reveal the tracking performance of FADI controller in the presence of high-order mismatched disturbances and actuator saturation. The trajectories of outputs are plotted in Fig. 10, and the curves of other states are depicted in Fig. 11 - Fig. 12. Observe that the output under FADI tracks the time-varying desired signal more accurately than the output under ABB. Additionally, x_2 and x_3 are still bounded under FADI, which demonstrates the stability conclusion in

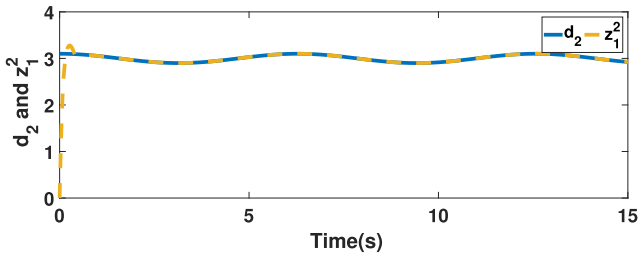

FIGURE 14. Trajectories of d_2 and its estimate z_1^2.

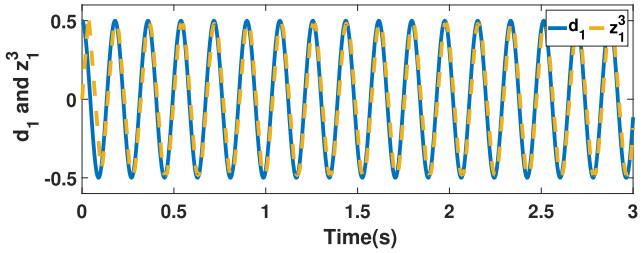

FIGURE 15. Trajectories of d_3 and its estimate z_1^3.

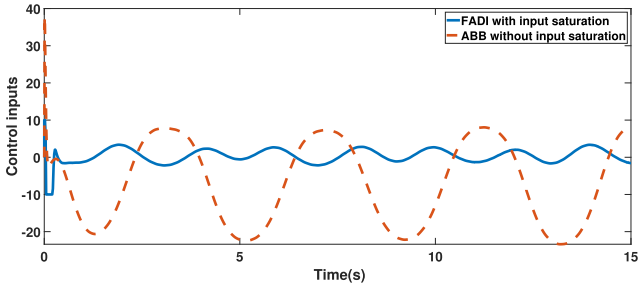

FIGURE 16. Time response of control inputs based on FADI and ABB.

Theorem 1. Fig. 10 - Fig. 15 illustrate that the estimates of states and high-order mismatched disturbances catch the objective signals immediately. Fig. 16 shows that the transient amplitude of FADI controller keeps in the required region during the entire tracking process. It can be concluded that the system steered by the FADI controller performs better than a system using the ABB controller, despite the input saturation.

VI. CONCLUSION

In this paper, we propose a novel disturbance-observer-based approximate dynamic inversion (ADI) control law for pure-feedback nonaffine-in-control nonlinear systems (PFNNSs) with high-order mismatched disturbances and actuator saturation. A modified ADI design method is developed taking consideration of actuator saturation. The augmented intermediate subsystem is constructed to compensate the difference between the input with and without saturation. The finite-time disturbance observers (FTDOs) are successfully utilized for the complete PFNNSs to estimate both states and high-order mismatched disturbances accurately and timely. The effectiveness of the proposed method is validated through the simulation results. For further research, we will investigate

approaches to extend the proposed control scheme to multi-input-multi-output systems.

REFERENCES

[1] J. Huang, M. Zhang, S. Ri, C. Xiong, Z. Li, and Y. Kang, "High-order disturbance-observer-based sliding mode control for mobile wheeled inverted pendulum systems," *IEEE Trans. Ind. Electron.*, vol. 67, no. 3, pp. 2030–2041, Mar. 2020.
[2] J. Yang, J. Su, S. Li, and X. Yu, "High-order mismatched disturbance compensation for motion control systems via a continuous dynamic sliding-mode approach," *IEEE Trans. Ind. Informat.*, vol. 10, no. 1, pp. 604–614, Feb. 2014.
[3] W. Zheng and M. Chen, "Tracking control of manipulator based on high-order disturbance observer," *IEEE Access*, vol. 6, pp. 26753–26764, 2018.
[4] B. Qiu, G. Wang, Y. Fan, D. Mu, and X. Sun, "Robust adaptive trajectory linearization control for tracking control of surface vessels with modeling uncertainties under input saturation," *IEEE Access*, vol. 7, pp. 5057–5070, 2019.
[5] W. He, Y. Dong, and C. Sun, "Adaptive neural impedance control of a robotic manipulator with input saturation," *IEEE Trans. Syst., Man, Cybern., Syst.*, vol. 46, no. 3, pp. 334–344, Mar. 2016.
[6] W. Gu, J. Yao, Z. Yao, and J. Zheng, "Robust adaptive control of hydraulic system with input saturation and valve dead-zone," *IEEE Access*, vol. 6, pp. 53521–53532, 2018.
[7] S. K. Maryam, "Dead-zone model-based adaptive fuzzy wavelet control for nonlinear systems including actuator saturation and dynamic uncertainties," *Int. J. Fuzzy Syst.*, vol. 20, no. 8, pp. 2577–2592, 2018.
[8] J. Gadewadikar, F. L. Lewis, K. Subbarao, K. Peng, and B. M. Chen, "H-infinity static output-feedback control for rotorcraft," *J. Intell. Robot. Syst.*, vol. 54, no. 4, pp. 629–646, Apr. 2009.
[9] B. Guo and Y. Chen, "Output integral sliding mode fault tolerant control for nonlinear systems with actuator fault and mismatched disturbance," *IEEE Access*, vol. 6, pp. 59383–59393, 2018.
[10] Z. Song and H. Li, "Second-order sliding mode control with backstepping for aeroelastic systems based on finite-time technique," *Int. J. Control Autom. Syst.*, vol. 11, no. 2, pp. 416–421, Apr. 2013.
[11] X. Fang, F. Liu, Z. Wang, and N. Dong, "Novel disturbance-observer-based control for systems with high-order mismatched disturbances," *Int. J. Syst. Sci.*, vol. 49, no. 2, pp. 371–382, Jan. 2018.
[12] R. Rashad, A. Aboudonia, and A. El-Badawy, "A novel disturbance observer-based backstepping controller with command filtered compensation for a MIMO system," *J. Franklin Inst.*, vol. 353, no. 16, pp. 4039–4061, Nov. 2016.
[13] A. Levant, "Higher-order sliding modes, differentiation and output-feedback control," *Int. J. Control*, vol. 76, nos. 9–10, pp. 924–941, Jan. 2003.
[14] S. Li, H. Sun, J. Yang, and X. Yu, "Continuous finite-time output regulation for disturbed systems under mismatching condition," *IEEE Trans. Autom. Control*, vol. 60, no. 1, pp. 277–282, Jan. 2015.
[15] X. Fang and F. Liu, "High-order mismatched disturbance rejection control for small-scale unmanned helicopter via continuous nonsingular terminal sliding-mode approach," *Int. J. Robust. Nonlinear Control*, vol. 29, no. 4, pp. 935–948, Mar. 2019.
[16] M. Rehan, M. Tufail, C. K. Ahn, and M. Chadli, "Stabilisation of locally Lipschitz non-linear systems under input saturation and quantisation," *IET Control Theory Appl.*, vol. 11, no. 9, pp. 1459–1466, 2017.
[17] A. Shams, M. Rehan, M. Tufail, C. K. Ahn, and W. Ahmed, "Local stability analysis and H∞ performance for Lipschitz digital filters with saturation nonlinearity and external interferences," *Signal Process.*, vol. 153, pp. 101–108, Dec. 2018.
[18] L. Zhang, M. Chen, Q.-X. Wu, and B. Wu, "Fault tolerant control for uncertain networked control systems with induced delays and actuator saturation," *IEEE Access*, vol. 4, pp. 6574–6584, 2016.
[19] R. Wang, H. Jing, J. Wang, M. Chadli, and N. Chen, "Robust output-feedback based vehicle lateral motion control considering network-induced delay and tire force saturation," *Neurocomputing*, vol. 214, pp. 409–419, Nov. 2016.
[20] S. Aouaouda and M. Chadli, "Robust fault tolerant controller design for Takagi-Sugeno systems under input saturation," *Int. J. Syst. Sci.*, vol. 50, no. 6, pp. 1163–1178, 2019.
[21] L. Tao and W. Lan, "Composite nonlinear feedback control for strict-feedback nonlinear systems with input saturation," *Int. J. Control*, vol. 92, no. 9, pp. 2170–2177, 2019.
[22] J. D. Boskovic, L. Chen, and R. K. Mehra, "Adaptive control design for nonaffine models arising in flight control," *J. Guid., Control, Dyn*, vol. 27, no. 2, pp. 209–217, Mar. 2004.
[23] X. Bu, G. He, and K. Wang, "Tracking control of air-breathing hypersonic vehicles with non-affine dynamics via improved neural back-stepping design," *ISA Trans.*, vol. 75, pp. 88–100, Apr. 2018.
[24] G. Sun, X. Ren, Q. Chen, and D. Li, "A modified dynamic surface approach for control of nonlinear systems with unknown input dead zone," *Int. J. Robust Nonlinear Control*, vol. 25, no. 8, pp. 1145–1167, May 2015.
[25] T. Sun and Y. Pan, "Adaptive control for nonaffine nonlinear systems using reliable neural network approximation," *IEEE Access*, vol. 5, pp. 23657–23662, 2017.
[26] S. Zhang, L. Kong, S. Qi, P. Jing, W. He, and B. Xu, "Adaptive neural control of unknown non-affine nonlinear systems with input deadzone and unknown disturbance," *Nonlinear Dyn.*, vol. 95, no. 2, pp. 1283–1299, Jan. 2019.
[27] C. Liu, H. Wang, X. Liu, and Y. Zhou, "Adaptive finite-time fuzzy funnel control for nonaffine nonlinear systems," *IEEE Trans. Syst., Man, Cybern., Syst.*, pp. 1–10, 2019.
[28] H. Liu, T. Zhang, and X. Xia, "Adaptive neural dynamic surface control of MIMO pure-feedback nonlinear systems with output constraints," *Neurocomputing*, vol. 333, pp. 101–109, Mar. 2019.
[29] Y. Pan and H. Yu, "Dynamic surface control via singular perturbation analysis," *Automatica*, vol. 57, pp. 29–33, Jul. 2015.
[30] H. Niu and Z. Geng, "Almost-global formation tracking control for multiple vehicles with disturbance rejection," *IEEE Access*, vol. 6, pp. 25632–25645, 2018.
[31] P. Forni and D. Angeli, "Perturbation theory and singular perturbations for input-to-state multistable systems on manifolds," *IEEE Trans. Autom. Control*, vol. 64, no. 9, pp. 3555–3570, Sep. 2019.
[32] N. Hovakimyan, E. Lavretsky, and C. Cao, "Dynamic inversion for multivariable non-affine-in-control systems via time-scale separation," *Int. J. Control*, vol. 81, no. 12, pp. 1960–1967, Dec. 2008.
[33] S. Yoo, "Adaptive control of non-linearly parameterised pure-feedback systems," *IET Control Theory Appl.*, vol. 6, no. 3, pp. 467–473, 2012.
[34] M. Asadi and H. T. Shandiz, "Adaptive control of pure-feedback systems with nonlinear parameterization via time-scale separation," *Int. J. Control Autom. Syst.*, vol. 15, no. 1, pp. 196–204, Feb. 2017.
[35] H. Yang and H. Pei, "A novel redesign framework to extend the application scope of a class of disturbance-rejection algorithms," *Int. J. Robust Nonlinear Control*, vol. 30, no. 1, pp. 321–337, 2019.
[36] H. K. Khalil, *Nonlinear System*, 3rd ed. Upper Saddle River, NJ, USA: Prentice-Hall, 2002.
[37] D. Dawson, J. Carroll, and M. Schneider, "Integrator backstepping control of a brush DC motor turning a robotic load," *IEEE Trans. Control Syst. Technol.*, vol. 2, no. 3, pp. 233–244, Sep. 1994.
[38] Y. Yang, J. Tan, and D. Yue, "Prescribed performance tracking control of a class of uncertain pure-feedback nonlinear systems with input saturation," *IEEE Trans. Syst., Man, Cybern., Syst.*, to be published.

HAO YANG received the B.S. and M.S. degrees from the Shaanxi University of Science & Technology, China, in 2010 and 2013, respectively. He is currently pursuing the Ph.D. degree with the School of Automation Science and Engineering, South China University of Technology, Guangzhou, China.

His research interests include singular perturbation theory, disturbance rejection, and robust control.

HAILONG PEI was born in 1965. He received the Ph.D. degree in automatic control from the South China University of Technology, Guangzhou, China, in 1992.

From 1997 to 1998, he did a Postdoctoral Research in the Chinese University of Hong Kong. He is currently a Professor with the School of Automation Science and Engineering, South China University of Technology, Guangzhou, China. His research interests include robot control, neural networks, nonlinear control, and so on.